Textures and Microstructures, 1991, Vols 14–18, pp. 85–90
Reprints available from the publisher
Photocopying permitted by license only

A REVIEW OF THE ANALYSIS OF LOCAL TEXTURE BY ELECTRON DIFFRACTION

R.A. Schwarzer
Institut für Metallkunde und Metallphysik der TUC,
Grosser Bruch 23, D-3392 Clausthal-Z., Germany

On-line measurement of pole figures with the TEM

Orientation measurements grain by grain with transmission or scanning electron microscopes yield comprehensive crystallographic and stereological data. Extremely fine-grain or deformed materials, however, are not accessible to single orientation measurements, since the grains may not be distinguished from each other, or the patterns are too diffuse for interpretation. Furthermore, the knowledge of pole figures rather than grain specific texture is often sufficient. This led to the development of a technique for the automatic measurement of pole figures with a TEM in selected area diffraction mode (SAD pole figures) [1), 2)]. The method is based on the same principles as the conventional transmission technique with x-ray diffraction. The specimen is tilted at small angular steps, $\Delta\beta$, around a preferred axis perpendicular to the primary beam direction (e.g. the rolling direction which is placed parallel to the goniometer axis), while the diffracted intensities are acquired along a selected Debye Scherrer ring by an electronic deflection of the diffraction pattern. Two automated acquisition techniques have been developed [2)]:

- The diffraction pattern is scanned circularly over a Faraday cup by a post-specimen deflection of the beam.
- The primary beam is deflected conically in front of the specimen, and the intensity values are measured from the diffraction pattern or dark-field images using the Faraday cup or the fluorescent screen.

The angle of specimen tilt, β, and the deflection angle, α, define a point (α,β) on the hkl pole figure for which the diffracted intensity $I(\alpha,\beta)$ is measured on the selected hkl ring. The corresponding pole density is represented graphically on the pole-figure plot by a specific colour out of a linear colour scale. Since the sample soon becomes impervious with steep inclination, the angle of tilt ranges up to only 45° or 60° in commercial microscopes, and SAD pole figures are incomplete showing a lens-shaped blind center. Local texture can be measured from areas as small as the specimen regions are selected by SAD (0.2 µm to 1.5 µm diam.), provided the number of sampled grains is statistically sufficient. SAD pole figures are best suited for the study of extremely fine grain or deformed materials.

Quantification of TEM pole figures and application

Two program options have been developed to interpret quantitatively the diffracted intensities in terms of pole-volume distribution[2)]. With the "analytical correction", allowance is made for the increase in diffracting volume and absorption when tilting the sample out of the direction of normal beam incidence. With the "experimental correction" the intensities of each Debye-Scherrer ring are normalized on its values at the intersections of the tilt axis, provided there is sufficient intensity. These reference values belong to

virtually the same point on the pole figure, due to the small Bragg angles in electron diffraction. Hence their variations, when tilting the sample, reveal the effects which do not originate from crystal texture. For random samples the residual pole-density fluctuations have proofed to be less than 10 % with both correction methods.

To give an example, SAD pole figures were measured from deformation and shear beands after 80% deformation of titanium by rolling [3]. Deformation bands, though only a few microns wide, show the usual crystal texture of titanium sheet known from x-ray measurement, whereas the texture of shear bands is distinctly different. The ideal orientation in deformation bands can be expressed by {00.1}<10.0> rotated around the rolling direction by about 40° out of the transverse direction (Figure 1a).The ideal orien-

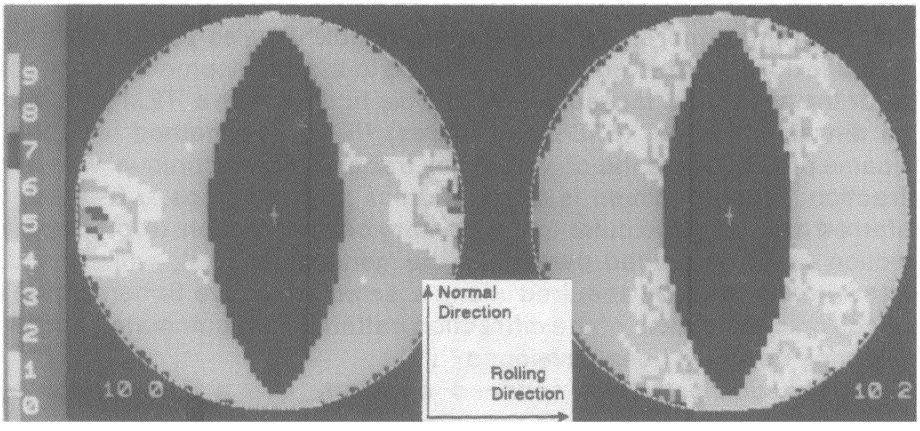

a) Deformation band

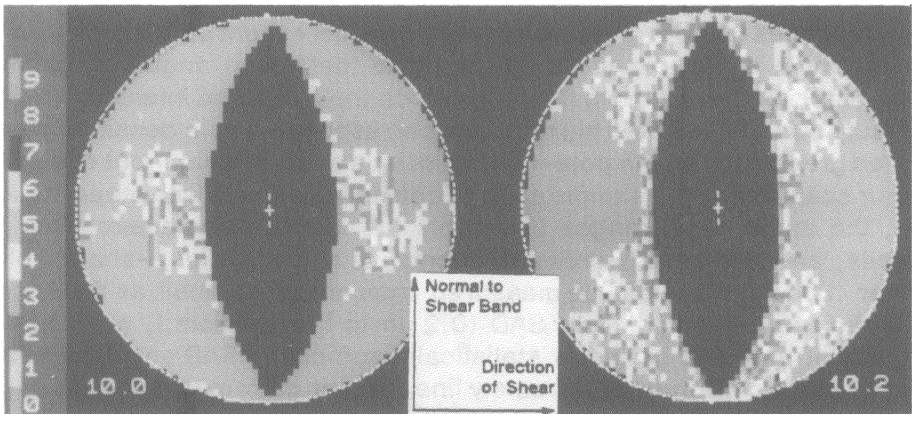

b) Shear band

Figure 1 SAD pole figures of 80% deformed titanium.

tation of a shear band can be described by crystals with their <10.0> axes parallel to the transverse direction. They are rotated by about 30° to 40° out of the rolling direction (Figure 1b) such that the grains are preferably orientated with their c-axes standing normal on the shear-plane.

The orientations of individual grains

Quantitative texture analysis is based up to now on the orientation distribution function (ODF). This concept suffers from two main shortcomings: ODF when computed from experimental pole figures is not unique, and the spatial arrangement of crystallites and intercrystalline interfaces is not considered. In many materials texture is not homogeneous over the whole workpiece, but varies if small volume sections are considered. This problem can be overcome by the measurement of individual orientations grain by grain.

Single orientations can be determined with unrivalled precision and resolution by lattice-plane imaging in high-resolution TEM. Due to the high expense in sample preparation and equipment, this method is mainly reserved for the study of single intergranual interfaces. Standard SAD electron spot patterns,on the other hand,suffer from an insufficient definition of the sampled area (> 0.5 µm), the low accuracy of orientation value (typical errors about 5°, unless tedious techniques are employed), and proneness to ambiguous indexing. More reliable results are obtained from microbeam diffraction (MBD) Kikuchi patterns (Figure 2) (transparent specimens, TEM) or reflection Kikuchi patterns (bulk specimens, SEM). The sampled area is defined on the specimen by the focussed stationary primary beam ("spot mode"). The diffracting volume ranges from some 10 nm width in thin foils to about 0.5 µm diam. on bulk samples. If neighbouring grains are studied, orientation differences less than 0.1° can be detected. When interpreting the crystal orientation with respect to the workpiece, a larger error than this may be introduced by misalignments of the sample and the microscope.

In the SEM the beam impinges on the sample at an angle of typically 30° from grazing incidence (Figure 3). Reflection Kikuchi patterns when recorded on an SEM are also called electron backscattering patterns (EBS) [4] or backscatter Kikuchi patterns [5]. For their acquisition, either a photographic plate or a fluorescent transmission screen is placed parallel to the incident beam, right in front of the tilted sample. In the latter arrangement patterns may be recorded with a high-gain TV camera or by photography through a window from outside. An advantage over image intensification and digital image store at TV frame speed is to first integrate the still pattern on the Peltier cooled sensor chip of a dedicated CCD camera and then to pass the improved pattern in a single scan [6] to the computer.

SAD channeling patterns are obtained in the SEM by rocking the electron beam on a selected region in the surface of a bulk sample. As a consequence of the large spherical lens aberrations and the need for rocking angles in excess of ± 5°, the illuminated sample area can be kept scarcely smaller than 5 µm in commercial microscopes. This is not sufficient for the study of deformed materials.

An outstanding advantage of texture measurement by electron microscopy is high local resolution and the ability of imaging the microstructure of the sampled region. The volume from which transmission Kikuchi patterns originate is at least one order of magnitude smaller than that of reflection Kikuchi patterns, and two orders of magnitude smaller than that of channeling patterns or reflection Kossel patterns. Distinct Kikuchi or chan-

neling patterns are only obtained when the diffracting volume is virtually a perfect crystal. So the degree of deformation sets a stringent limit on the usefulness of the SEM. The preparation of thin foils for the TEM, however, is tedious, and only a small area of the sample is sufficiently transparent

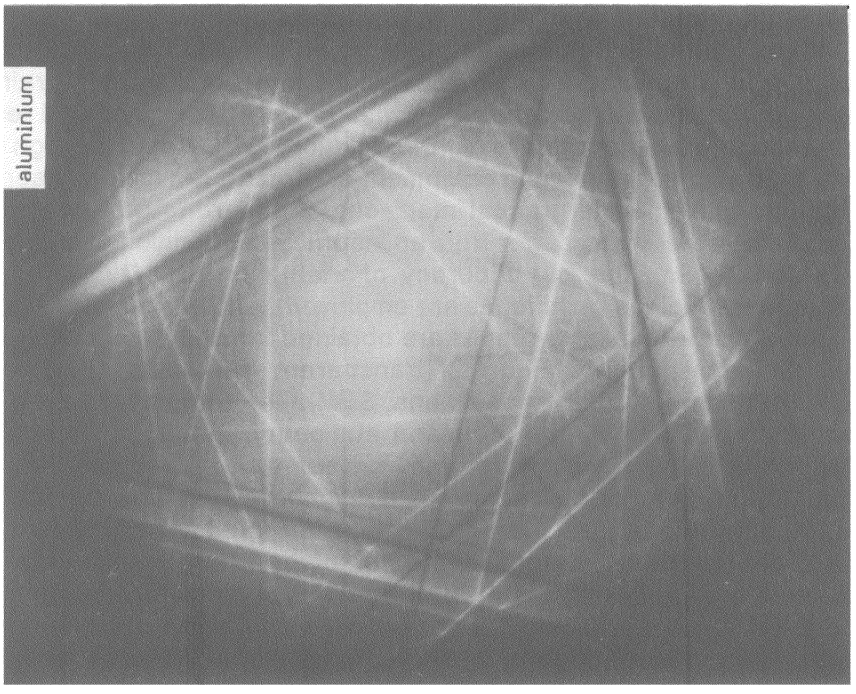

Figure 2 Transmission Kikuchi pattern from aluminium. (300 kV accelerating voltage)

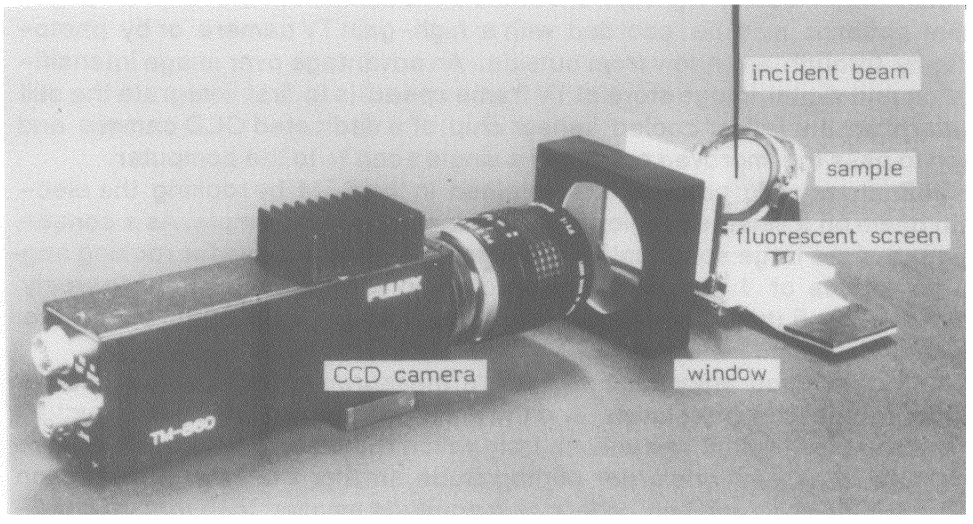

Figure 3 Setup for the acquisition of reflection Kikuchi patterns using a CCD camera.

which may not be representative for the whole workpiece. The SEM is less suited for the study of fine-grain or deformed materials. The main field of application of reflection Kikuchi patterns are materials with grain sizes in the micron range, the study of large sample areas, the investigation of secondary recrystallization and grain coarsening. The domain of channeling patterns will be single and polycrystal semiconductors.

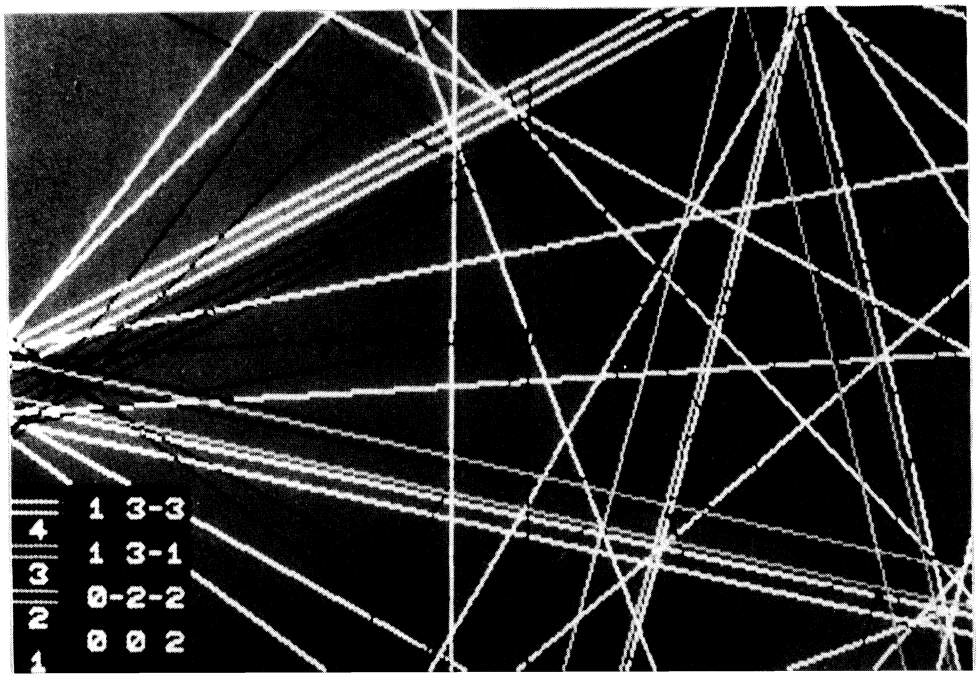

Figure 4 Kikuchi map for aluminium (solution for Figure 2).

On-line interpretation of electron diffraction patterns

A significant advance is to perform measurement and interpretation of diffraction spot [7], transmission Kikuchi or channeling [8] and reflection Kikuchi [9] patterns on-line with a microcomputer linked to the microscope. Precise determination of crystal orientations from Kikuchi or channeling patterns is based on the sharpness of the lines and on the fact that they rigidly follow any rotation or tilt movement of the crystal. So simply the positions of Kikuchi lines must be measured in the patterns. On-line interpretation by measurement of Kikuchi lines can do without any operator's knowledge of crystallography, whereas full advantage is taken of the visual perception of man. Measurement and interpretation is accomplished in less than 1 minute for cubic symmetry[8].Time for indexing increases,however, with lower crystal symmetry. In order to exclude false orientations due to inaccurate measurement and to discriminate [uvw] from [$\bar{u}\bar{v}\bar{w}$] directions, it is recommended to compute a Kikuchi map from each possible solution (Figure 4), and to check it immediately with the actual pattern.

Diffuse bands rather than sharp lines are usually found in reflection Kikuchi patterns when recorded with a TV camera. Then indexing can no longer make use of Bragg's equation. Accuracy of crystal orientation measurement is markedly reduced to less than 1°, if clear Kikuchi lines are not available. The range of accepted diffraction angles, however, extends over more than ± 20°, and a large section of the standard orientation triangle is covered by a single reflection pattern. The interpretation may be accomplished by a trained operator who may identify some principal crystallographic zone axes and pass their positions to a computer [5]. This simple indexing method by visual inspection is practicable for crystals with high symmetry (cubic, hexagonal) [9].

A fully automatic method of indexing of Kikuchi patterns is in principle feasible, and some efforts have been made [10], [11]. The basic problem lies in the automatic recognition of principal zone axes or bands in reflection Kikuchi patterns which show a very low contrast (typically < 4%), low intensity at a high level of noise, diffuse lines or bands, and high non-uniform background. The first approach to automation is to improve pattern quality. Optimized hardware seems necessary, e.g.

- efficient image detection (phosphor or YAG screen matched to spectral response of camera; (tapered) fiber optic rather than lens system; direct detection of the electron signal rather than the fluorescent image).
- energy filtering to exclude high-loss electrons. Some improvement of contrast has been reported for channeling patterns [12].
- analogue image store on cooled CCD sensor chip; slow scan, broad band-pass amplification of the image in order to reduce noise and to increase dynamics.
- high-performance frame grabber boards to support sophisticated real time software (subtraction of "empty" images (background), image convolution and filter functions).

The goal is to enable the unattended collection of a statistically great number of orientations by a raster scan over a sample in the SEM.

References

1. Humphrey, F.J. (1984), Proc. ICOTOM 7, 771-776.
2. Schwarzer, R. (1985), Beitr. elektronenmikr. Direktabb. Oberflächen (BEDO) 18, 61-68.
3. Schwarzer, R.A. (1988). Proc. EUREM 88, Inst. Phys. Conf. Series No 93, Vol.2, pp. 23-24.
4. Venables, J.A. and Harland, C.J. (1973), Phil. Mag. 27, 1193-1200.
5. Dingley, D.J. (1984), SEM 1984/II, 569-575.
6. Schwarzer, R. (1989), BEDO 22, 279-282.
7. Carr, M.J. (1982), JEOL news 20E, 7-9.
8. Weiland, H. and Schwarzer, R. (1985), BEDO 18, 55-60.
9. Dingley, D.J. (1990), ICOTOM 9 this volume
10. Ishida, Y., Mori, M., Arimoto, A. and Onoe, M. (1981), Proc. ICOTOM 6, 601-608.
11. Juul Jensen (1990), D. and Schmidt, N.H., ICOTOM 9 , this volume
12. Rösch, G. (1987), PhD Thesis, University of Tübingen.